Chemical Science

EDGE ARTICLE

The contribution of non-classical $CH_{ax}\cdots OC$ hydrogen bonds to the anomeric effect in fluoro and oxa-methoxycyclohexanes

Received 00th January 20xx,
Accepted 00th January 20xx

DOI: 10.1039/x0xx00000x

Bruno A. Piscelli,[a] David O'Hagan,[b]* and Rodrigo A. Cormanich[a]*

In this theory study we demonstrate the dominance of non-classical 1,3-diaxial $CH_{ax}\cdots OC$ hydrogen bonds (NCHBs) dictating a 'pseudo' anomeric effect in selectively fluorinated methoxycyclohexanes and also influencing the axial preference in the classical anomeric exhibitor 2-methoxytetrahydropyran, a phenomenon which is most often described as a consequence of hyperconjugation. Analogues of methoxycyclohexane where ring CH_2's are replaced by CF_2 can switch to an axial preference and theory methods (NBO, QTAIM, NCI) indicate the dominance of 1,3- $CH_{ax}\cdots OMe$ interactions over hyperconjugation. For 2-methoxytetrahydropyran, it is revealed that the global contribution to the anomeric effect is from electrostatic interactions including NCHBs, not hyperconjugation, although hyperconjugation ($n_O \rightarrow \sigma^*_{CO}$ or $n_O \rightarrow \sigma^*_{CC}$) remains the main contributor to the exo-anomeric phenomenon. When two and three ether oxygens are introduced into the ring, then both the NCHB interactions and hyperconjugative contributions become weaker, not stronger as might have been anticipated, and the equatorial anomers progressively dominate.

Introduction

The anomeric effect in the prototype example 2-methoxytetrahydropyran **1**, recognises that the OMe group prefers to adopt an axial rather than an equatorial orientation contrary to classical effects in monosubstituted cyclohexanes. The origin of the anomeric effect has been debated for several decades, with insights from different perspectives giving rise to the development of competing working hypotheses. These various interpretations derive from steric, electrostatic and hyperconjugative considerations. The most widely discussed explanation for the anomeric effect invokes hyperconjugation.[1,2,3,4,5] In the case of 2-methoxytetrahydropyran **1** this is facilitated in the axial conformer where there is an antiperiplanar relationship between a lone pair of the (*endo*) ring oxygen 2p-type and the antibonding orbital of the exocyclic C-O bond ($n_O \rightarrow \sigma^*_{CO}$ overlap) (Figure 1a). This is reciprocated by hyperconjugation between a lone pair of the (*exo*) methoxyl oxygen and the endocyclic bond ($n_O \rightarrow \sigma^*_{CO}$ overlap). These interactions constitute the *endo* and *exo* anomeric effects respectively. However, there is also more efficient dipole-dipole relaxation between the two C-O bonds in the axial conformer and thus electrostatics also favour an axial preference for the OMe substituent (Figure 1b), which was pointed out to be the effect that rules axial preference by Mo *et al.* by applying the block-localized wavefunction method.[6] Then there is greater n_O/n_O steric hindrance in the equatorial conformer, which has parallel 2p-type n_O filled orbitals again favouring the axial conformer (Figure 1c).[7,8,9,10] Finally and most recently, non-classical hydrogen bonds (NCHBs) such as transannular $CH_{ax}\cdots OC$ interactions have been proposed by Nishio[11] and supported by Wiberg[12] and Cuevas[13] which introduce a further electrostatic factor. NCHBs occur when an electronegative atom (in this case O) interacts with a covalently bound X-H hydrogen but where the X atom is of moderate to low electronegativity (in this case C).[14,15] These authors[11-13] and particularly Wiberg[12] have argued an increasing significance for electrostatic interactions in determining the anomeric effect with a decreasing emphasis on the more widely propagated hyperconjugation model. It is the NCHB interactions which form the focus of this work, where we deconvolute [using Natural Bond Orbital (NBO) analysis,[16] Quantum Theory of Atoms in Molecules (QTAIM)[17] and Non Covalent Interactions (NCI)[18]] their contributions relative to hyperconjugation, and provide quantitative support to this revision, in an approach which extends from a deeper analysis of our recent observations of 'pseudo' anomeric effects in cyclohexanes **2**, **4**, **5** and **8**.[19] The conformational preference of methoxycyclohexane is equatorial (by ~ -0.45 kcal mol^{-1}),[19] but

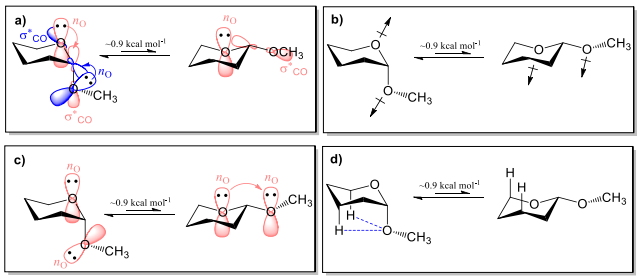

[a] University of Campinas, Chemistry Institute, Monteiro Lobato Street, Campinas, Sao Paulo, Brazil - 13083-862, E-mail: cormanich@unicamp.br
[b] School of Chemistry, University of St Andrews, North Haugh, St Andrews, KY16 9ST, UK. E-mail: do1@st-andrews.ac.uk

Electronic Supplementary Information (ESI) available: Computational details, benchmark results, NBO, QTAIM and NBO details and Cartesian coordinates for all molecules. See DOI: 10.1039/x0xx00000x

Figure 1. Representation of the effects used to explain the origin of the axial preference in 2-methoxytetrahydropyran. **a)** $n_O \rightarrow \sigma^*_{CO}$ Hyperconjugation in the *endo* (pink) and *exo* (blue) anomeric effects, **b)** Dipole moment minimisation, **c)** n_O/n_O 2p-type steric repulsion and **d)** CH···OMe stabilising interactions.

it can be strongly influenced by the strategic placement of fluorine atoms. Both experiment and theory have demonstrated that cyclohexane **2**, which has a CF_2 group in place of the ring oxygen relative to tetrahydropyran **1**, prefers an axial geometry (by 1.22 kcal mol^{-1}) with a very similar bias in energy to **1** (1.10 kcal mol^{-1}) as illustrated in Figure 2. Perhaps more surprisingly cyclohexane **4** with a distal CF_2 group, also prefers an axial geometry (0.74 kcal mol^{-1}) and the preference is increased in **5** (2.06 kcal mol^{-1}) where there are two CF_2 groups, and it increases again in **8** (3.04 kcal mol^{-1}), with three CF_2 groups. These results pointed towards the importance of CH_{ax}···OC NCHBs, dictating the conformational preferences in cyclohexanes **2**, **4**, **5** and **8**, and where increasing the number of CF_2 groups increases the axial preference. Consistent with this analysis, when the electropositive H_{ax} atoms are replaced by electronegative F_{ax} atoms, then the equatorial conformers become more stable (eg. **3** and **7**), to avoid CF_{ax}···O(Me) electrostatic repulsions.[19]

In this paper we explore these phenomena further. We anticipated that positioning additional equatorial F atoms at positions 3 and 5 as in methoxycyclohexane **10** would further increase this axial preference, however we disclose now that the calculated Gibbs free energies for this equilibrium unexpectedly decreases, and all the equilibria for cyclohexanes **9-12** indicate that the axial preference is much more attenuated relative to **2**, **4** and **5**, and in the case of **10-12** the equatorial conformers are close to isoenergetic with the axial conformers. The study was then extended to oxa-methoxycyclohexanes which display more classical anomeric effects.

Results and Discussion

NBO analysis was used to deconvolute the relative contributions of hyperconjugation, electrostatics and steric effects. NBO[16] analysis contracts the molecular orbitals into natural bonding orbitals, localising every electron in the molecule to bonds and lone pairs and reproducing a Lewis representation of the molecule. Nevertheless, NBO also generates unoccupied, antibonding orbitals that can accept electron density, leading to electron delocalisation and therefore, hyperconjugative effects. In this way by deleting all unoccupied orbitals, it is possible to calculate the energy of a hypothetical molecule [ΔE(L)] where all bonding orbitals have an occupancy of 2 electrons and the distribution is governed only by classical effects. A comparison of this energy with the electronic energy of the molecule [ΔE(T)] offers a measure of the non-Lewis contribution, and therefore the contribution of hyperconjugative effects [(ΔE(NL)]. Table 1 summarizes those energies for molecules **1-18**, as well as their Natural Coulomb Energy [(ΔE(NCE)], which takes into account the Coulomb equation ($E_{NCE} = \Sigma_{A,B}\ Q_A Q_B / R_{AB}$) using atomic charges from NPA for the calculation of the molecular electrostatic energy,[20] and the energy obtained from the Natural Steric Analysis [(ΔE(NSA)],[21] which gives the energies associated with intramolecular steric repulsions.

As previously observed,[19] the stability of methoxycyclohexanes **1-5** and **7-8** rely on Coulomb electrostatic interactions. When ΔE(NCE) is positive, the equilibria favour the axial anomer and in general, the more positive the NCE energy the higher this anomeric preference. For instance, ΔE(NCE) is +8.84 and +28.34 kcal mol^{-1} for **2** and **8**, respectively, and the ΔG penalty for placing the methoxyl group in an equatorial orientation in these cases is 1.22 and 3.40 kcal mol^{-1}, respectively. A similar trend is observed for **9** with a 0.59 kcal mol^{-1} axial preference and a +4.71 kcal mol^{-1} NCE energy. However, for the series **10-12**, despite additional geminal F atoms in the ring, the electrostatic contribution increasingly supports an equatorial preference for OMe. Counterintuitively, the atomic charges obtained from the natural population analysis (NPA; see Table S60) on the H_{ax} atoms at positions 3 and 5 in these rings are more positive when there

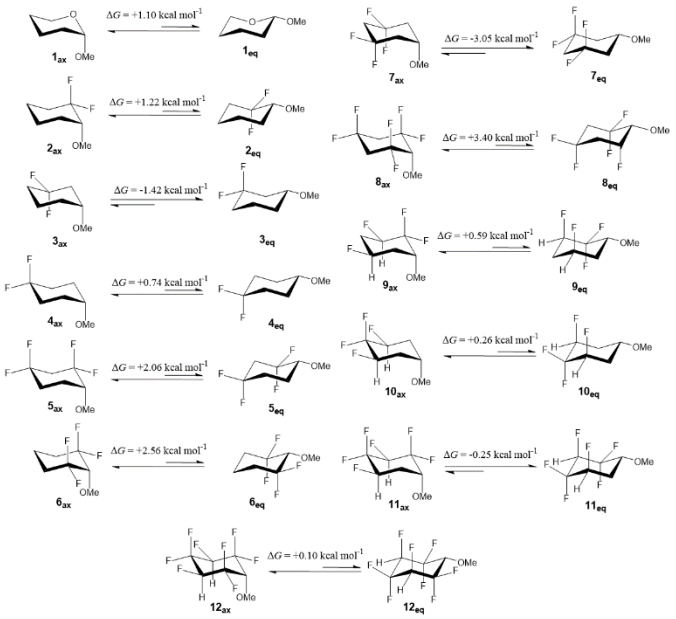

Figure 2. Calculated ax/eq preferences for compounds **1-12** calculated at the M06-2X/aug-cc-pVTZ level in terms of Gibbs free energies (kcal mol^{-1}).

	ΔE(T)	ΔE(L)	ΔE(NL)	ΔE(NCE)	ΔE(NSA)
1	1.39	4.11	-2.72	0.41	-1.39
2	1.36	9.16	-7.80	8.84	-1.61
3	-0.80	-1.01	0.21	-1.37	-2.43
4	1.08	3.73	-2.65	3.50	-3.38
5	2.28	10.61	-8.33	14.71	-1.66
6	2.96	13.34	-10.38	22.18	-0.31
7	-2.53	-5.84	3.31	-5.54	-0.62
8	3.81	14.50	-10.69	28.34	-0.81
9	0.79	5.19	-4.40	4.71	0.01
10	0.60	-3.11	3.71	-0.75	-1.79
11	0.41	-2.41	2.83	-2.01	-1.57
12	0.47	-2.33	2.80	-0.31	-1.50
13	-0.35	-3.26	2.91	-9.16	-2.51
14	-0.25	5.51	-5.76	-0.04	-2.84
15	1.26	7.38	-6.12	5.03	-1.71
16	0.90	2.88	-1.98	0.25	-1.27
17	-1.59	-4.16	2.57	0.82	-4.29
18	0.03	5.90	-5.87	2.18	-0.83

Table 1. NBO analysis relative energies (in kcal mol^{-1}) obtained at the M06-2X/aug-cc-pVTZ theoretical level for compounds **1-18**, where **ΔE(T)** is the electronic, **ΔE(L)** the Lewis, **ΔE(NL)** the non-Lewis, **ΔE(NCE)** the electrostatic and **ΔE(NSA)** the steric energies. Positive values represent a preference for the axial conformer and negative ones for the equatorial conformer.

are no geminal F atoms. This appears to be the result of an inversion in the atomic charge of the C3 and C5 carbons, since both are negatively charged in **2**, **4**, **5** and **8**, however they become positively charged when F atoms are attached in **9-12**. Considering that the Coulombic potential decays quadratically with the distance, it appears to be more favourable to reduce the positive atomic charges on the 3,5-H_{ax} atoms in order to minimise short-range 1,2-$^{\delta+}$C-$^{\delta+}$H repulsions, than to increase their charge to accommodate long-range NCHB interactions with the methoxyl group. Hence, the NCE

interactions show that the NCHBs are much weaker when there are geminal F atoms attached to C3 and C5 (~15.5 kcal mol^{-1} in **12$_{ax}$**) compared to their lesser fluorinated analogues (eg. ~18.2 kcal mol^{-1} in **8$_{ax}$**).

A significant interaction in the equatorial conformers of **9**-**12** occurs between the C3-F$_{ax}$/C5-F$_{ax}$ fluorines and the electropositive C1-H$_{ax}$ hydrogen, geminal to the OMe group. NCI iso-surfaces show that there is an attractive Van der Waals interaction between these axial fluorines (3,5-F$_{ax}$) and the C1-H$_{ax}$ hydrogen. It emerges from the NCE analysis, that these CF$_{ax}$···H$_{ax}$C interactions range from between -8.6 to -10.0 kcal mol^{-1} in stabilisation energy, depending on the nature of the local electron-withdrawing CF$_2$ groups influencing the electropositive charge on H$_{ax}$ or the electronegative charge on F$_{ax}$.

The importance of electrostatic interactions in stabilising the axial conformers in **1**, **2**, **4**, **5**, **8** and **9** is further supported by their calculated Gibbs free energy equilibria values in solvents of increasing polarity. As shown in Table S58 there is an energy penalty of 1.22 kcal mol^{-1} in the gas-phase for placing the OMe group in an equatorial position in **2**. This is 3.40 kcal mol^{-1} in the case of **8**. However, this energy difference shrinks gradually through $CHCl_3$, CH_2Cl_2 and acetone, as the intramolecular electrostatic interactions are weakened in the more progressively polar solvents. The anomeric preference in acetone decreases to 0.20 kcal mol^{-1} and 1.12 kcal mol^{-1} in **2** and **8**, respectively.

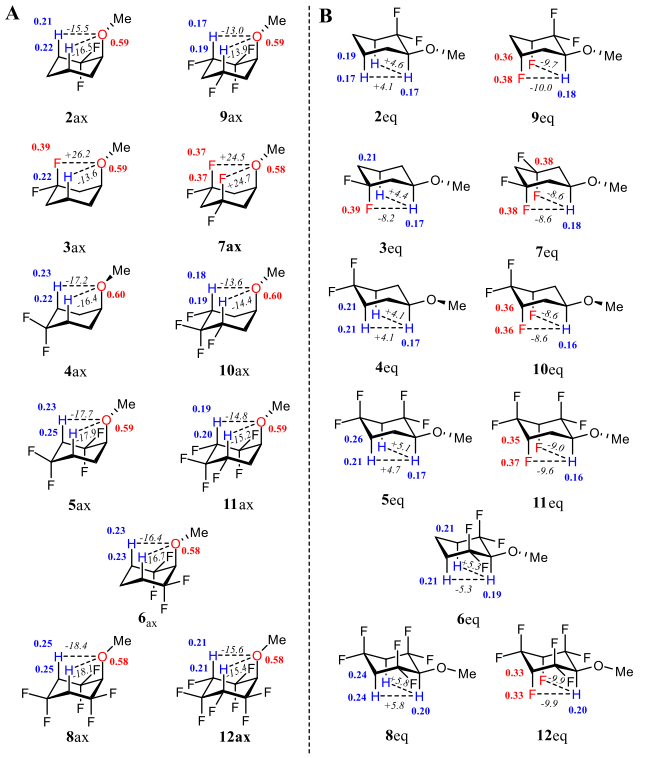

Figure 3. Calculated NPA atomic charges in atomic units (blue = positive, red = negative) at the M06-2X/aug-cc-pVTZ level and with electrostatic interactions in kcal mol^{-1} (in italics, negative represent stabilizing and positive represent destabilizing) for compounds **2**-**12**. **A:** In the axial conformers, the positioning of equatorial F atoms at C3 and C5 of the ring make the axial H atoms less positive, weakening NCHBs. **B:** F atoms at positions C3 and C5 stabilise interactions with C1-H$_{ax}$ in the equatorial conformers.

In contrast to that observed for compounds **1**-**8**, hyperconjugative effects, and particularly the 3,5-$\sigma_{CHax} \rightarrow 4\text{-}\sigma^*_{CFax}$ interactions, govern the higher electronic stability of the axial over the equatorial conformers in **10**-**12**. Two $\sigma_{CHax} \rightarrow \sigma^*_{CFax}$ are possible in an axial conformer, whereas these are replaced by $\sigma_{CFax} \rightarrow \sigma^*_{CFax}$ in the equatorial conformers (Figure S6). Because of the higher electron donating character of a σ_{CH} over a σ_{CF} orbital, hyperconjugative interactions are stronger in the axial conformers. This is evident in the ΔE(NL) values which indicate axial stabilisation of the methoxy group by 3.71 kcal mol^{-1}, 2.83 kcal mol^{-1} and 2.80 kcal mol^{-1} in **10**, **11** and **12**, respectively.

The study was now extended to oxa-heterocycles **13**-**18** which were selected to contain up to three ether oxygens relative to the original methoxycyclohexane ring system and to include systems such as **15**, **16** and **18** which should display classical anomeric phenomenon. The structures and the equilibria of analogues **13**-**18** are represented in Figure 4 and calculated energy values are shown in full in Table S58. Most notably, despite the structural similarities between the two classes of compounds, the anomeric preferences for the oxygenated molecules are very different to that observed for the fluorocyclohexane analogues. Although **1** and **2** have approximately

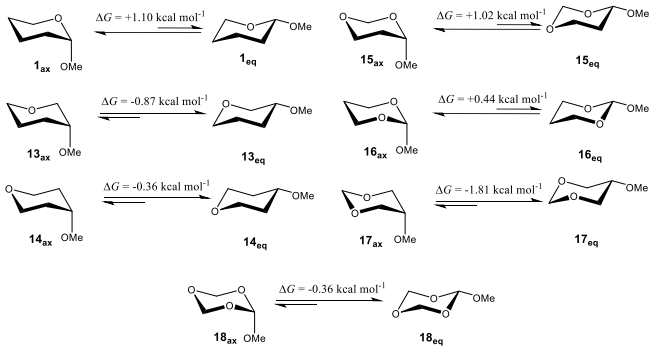

Figure 4. Calculated ax/eq preferences for compounds **1** and **13**-**18** calculated at the M06-2X/aug-cc-pVTZ level in terms of Gibbs free energies (kcal mol^{-1}).

the same interconversion barriers (1.10 and 1.22 kcal mol^{-1}, respectively), the same pattern is not observed for analogues **4** and **14**, where the former prefers the axial conformer (by 0.74 kcal mol^{-1}) and the latter the equatorial conformer (by 0.36 kcal mol^{-1}). Also, the axial preference of 2.06 kcal mol^{-1} in **5** decreases to 1.02 kcal mol^{-1} in the oxygenated analogue **15**. Even more curious is the observation that **18** prefers the equatorial conformer, when its fluorinated counterpart **8** has a large axial preference (by 3.40 kcal mol^{-1}). It appears that CH$_{ax}$···OC NCHB interactions are less important for these oxygenated ether analogues. A deconvolution of the total energy contributions for the oxygenated analogues using NBO analysis (Table 1), reveals an overall decrease in the electrostatic ΔE(NCE) contribution including NCHB interactions. For instance, the CH$_{ax}$···OC interactions are approximately 12-15 kcal mol^{-1} for **1**, 12 kcal mol^{-1} for **14** and only 10-12 kcal mol^{-1} for **15** and **18** (Figure 5). These same interactions are in the range of 15.5-18.4 kcal mol^{-1} for **2**, **4**, **5** and **8** and increase with the number of CF_2 groups in the molecule (Figure 3). It is noteworthy that in **18**, which contains three ether oxygens, and where it might be expected to show the strongest CH$_{ax}$···OC NCHBs, as observed with the three CF_2 groups in **8**, then the opposite behaviour is observed. This is now rationalized by the charge on the H$_{ax}$ atoms, which are significantly less positive in **13**-**15** and **18** and contrasts with the trend observed for **2**, **4**, **5** and **8**. The H$_{ax}$ atom become progressively less positive as the number of ether oxygens increase, as can be observed by comparing the H$_{ax}$ atom charges in **1$_{ax}$** (+0.17-0.20 au), **15$_{ax}$** (+0.14 au with two ring O atoms) and **18$_{ax}$** (+0.14-0.15 au with three ring O atoms) in Figure 5. The strongest NHCBs are observed in **1** (15.2 kcal mol^{-1}) and **13$_{ax}$** (15.8 kcal mol^{-1}) systems where there are H$_{ax}$ atoms that are not geminal to O atoms. It is noteworthy that other methods

for calculating atomic charges such as Chelp,[22] ChelpG,[23] QTAIM,[17] Hirshfeld (CM5),[24] MK[25,26] and Mulliken[27] give different magnitudes (Tables S59-S65). Most notably CHelpG predicts lower relative values than NPA (Figure S9 in the ESI), with all atoms much less positively or negatively charged. Indeed, the H_{ax} atoms show larger positive values relative to NPA, but CHelpG calculates very similar values for these same atoms, and particularly for the oxa-heterocycles. One can understand why H_{ax} atoms are less positively charged in the oxygenated analogues by investigating hyperconjugative interactions involving the σ^*_{CHax} orbitals as acceptors (Figure 6). In the axial conformers of **1** and **13-18** there are $n_O \rightarrow \sigma^*_{CHax}$ hyperconjugative interactions in the range of 5.9-8.0 kcal mol^{-1}, which indicates that the vicinal O atoms are donating charge to the H_{ax} atoms, and consequently decreasing their positive charge and weakening the strengths of the electrostatic $CH_{ax}\cdots$OC NCHB interactions. Moreover, $^{\delta-}O^{\delta-}O$ destabilizing electrostatic interactions between the ring oxygen(s) and the methoxyl oxygen (Figure 6) are minimized if the O atoms donate charge to H_{ax} atoms through hyperconjugation. This makes the H_{ax} atoms less positively charged, weakening $CH_{ax}\cdots$OC NCHB strengths, and at the same time decreasing $^{\delta+}C^{\delta+}H_{ax}$ and $^{\delta-}O^{\delta-}O$ electrostatic repulsions. Thus, the balance between electrostatic stabilisation/destabilisation is modulated by hyperconjugation.

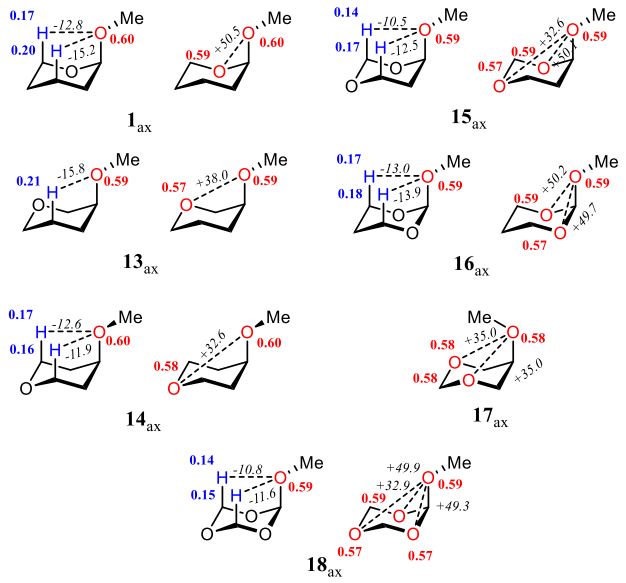

Figure 5. Calculated NPA atomic charges in atomic units (blue = positive, red = negative) at the M06-2X/aug-cc-pVTZ level and with electrostatic interactions in kcal mol^{-1} (in italics, negative represent stabilizing and positive represent destabilizing) for molecules **1** and **13**-**18**.

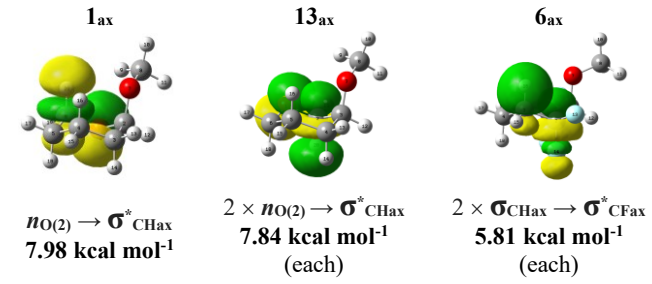

Figure 6. Hyperconjugative interactions in compounds **1** and **13** between ring O atoms and σ^*_{CHax} donate charge to H_{ax} and thus are responsible for lowering the energy of NCHBs in oxygenated compounds, while in **6** the $\sigma_{CHax} \rightarrow \sigma^*_{CFax}$ hyperconjugation withdraws charge from H_{ax} and thus strengthen the NCHBs. Interaction energies were calculated at the M06-2X/aug-cc-pVTZ theoretical level.

The equatorial conformer of **17** is significantly preferred over the axial conformer by 1.81 kcal mol^{-1} although the preference is reduced by comparison with tetrafluorocyclohexane **7**, which has an equatorial preference of 3.05 kcal mol^{-1}. This comparative reduction arises because in **17$_{ax}$** the methoxy group is directed toward the ring, as observed in the potential energy surfaces in Figure S5, enabling NCHB interactions between the ring O atoms and two of the methoxyl H atoms. The characterization of this interaction as NCHBs is supported by the formation of bond critical points (BCP) in QTAIM analysis, connecting the bridging atoms and by blue-coloured isosurfaces in NCI (Figure 7). The formation of such stabilising interactions is partially countered by steric repulsion as evidenced by the high value of ΔE(NSA) in **17** (Table 1).

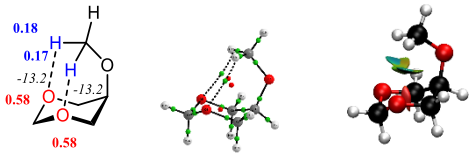

Figure 7. From left to right: 17 calculated NPA atomic charges in atomic units (blue = positive, red = negative) at the M06-2X/aug-cc-pVTZ level. Electrostatic interactions are in kcal mol^{-1} (in italics, negative represent stabilizing); QTAIM molecular graph: bond critical points (BCP, green) and ring critical points (RCP, red); NCI isosurfaces using reduced density gradient (RDG) = 0.5 and blue-green-red color scale ranging from -0.02 < sign(λ_2)ρ(r) < 0.02 a.u.

An interesting outcome here is the significant difference in energy for the axial preference between analogues **6** (2.56 kcal mol^{-1}) and **16** (0.44 kcal mol^{-1}) (see Fig 2 and Fig 4). The H_{ax} atoms are much less positively charged in **16** weakening the $CH_{ax}\cdots$OC NCHB interactions (13.0-13.9 kcal mol^{-1} for **16** and 16.4-16.7 kcal mol^{-1} for **6**) and as a result tetrafluorocyclohexane **6** has a much higher axial preference as indicated by ΔG in Figures 2 and 4. Furthermore, **1** has a greater axial preference than **16**, despite **16** having an additional oxygen with a capacity to participate in a $n_O \rightarrow \sigma^*_{CO}$ hyperconjugative interaction. This is contrary to expectation unless it is realised that the axial preference in **1** is dominated by electrostatics rather than hyperconjugation as is illustrated by the ΔE(NL) values in Table 1. Although the $n_O \rightarrow \sigma^*_{CO}$ hyperconjugative interactions in **1** and **16** are locally stabilising, the total molecular hyperconjugation contribution, ΔE(NL) actually favours an equatorial conformation in both compounds by ~2.0-2.7 kcal mol^{-1}. It is the larger overall electrostatic contribution that dictates the axial outcome. This is contributed by the strength of the 3-$CH_{ax}\cdots$OC NCHB interactions in **1** (15.2 kcal mol^{-1}) and to a lesser degree in **16** (13.9 kcal mol^{-1}) as illustrated in Figure 5. This outcome arises in turn from the less positive atomic charge on the 3-C-H_{ax} hydrogens in **16** due to neutralising $n_O \rightarrow \sigma^*_{CHax}$ hyperconjugative interactions from the additional O atom. The NCHB interaction values and H_{ax} atomic charges reduce even further in **18**, which has a third oxygen atom, and the overall bias now is unexpectedly towards an equatorial preference. In this way, NBO indicates that electrostatics are the main driving force for all compounds in this work that prefer the axial geometry as suggested by the electrostatic contribution [ΔE(NCE)] in Table 1; and that the fluorinated analogues have higher axial preferences because their H_{ax} atoms are more positively charged than in the oxa-heterocycles, thus forming stronger NCHBs.

Moreover, the effect of ring distortion between axial and equatorial conformers was evaluated (Cremer-Pople puckering coordinates[28]) as a potential contributor to the equilibria for all of the compounds studied (Table S66 in the Supporting Information). However, the θ the Q values are almost invariant between the

equatorial and axial conformers, and we conclude that relative ring puckers are not significant here.

Finally, we examined the contribution of NCHBs to the *exo*-anomeric effect particularly as it has been shown experimentally that the *exo*-anomeric effect has a more dominant hyperconjugative contribution than the *endo*-anomeric effect.[29] The *exo*-anomeric effect, considers the methyl group orientation of the OMe group in an axial conformation. This can be observed in Figure 8 which presents rotational energy curves for **1**$_{ax}$ and **2**$_{ax}$. The preferred dihedral angles for H-C-O-Me in an anomeric situation such as prototype **1**, fall in the range of 30-60° consistent with hyperconjugative interactions between a lone pair of the methoxyl O and the σ^*_{CO} antibonding orbital. When the angle is at 300° then the OMe methyl group, rather than an oxygen lone pair, occupies the anti-periplanar hyperconjugative site, disabling the $n_O \rightarrow \sigma^*_{CO}$ interaction. Optimal hyperconjugations are found in **1**$_{ax}$ and **15**$_{ax}$ (15.0-16.0 kcal mol^{-1} of stabilisation) at ~50° as expected, and in the case of the CF_2 containing cyclohexanes, less strong $n_O \rightarrow \sigma^*_{CC}$ interactions are found in **2**$_{ax}$, **5**$_{ax}$ and **13**$_{ax}$ (7.8-10.7 kcal mol^{-1}), at a slightly narrower angle of ~30° (see Figure S8). Interestingly **1**$_{ax}$ and **15**$_{ax}$ show a deep minimum at 50° consistent with a *gauche* preference, and then there is a barrier of about 4 kcal mol^{-1} at 300° where $n_O \rightarrow \sigma^*_{CO}$ interactions are disabled. It should be noted that both *gauche* orientations continue to accommodate $CH_{ax}\cdots OC$ NCHB interactions. The difference in the energies of these two interactions is ~2.0 kcal mol^{-1}, therefore this suggests that hyperconjugation contributes at least 50% (another 2.0 kcal mol^{-1}) to the *exo*-anomeric effect in prototype **1**$_{ax}$ and in **15**$_{ax}$. For the CF_2 systems **2**$_{ax}$ and **5**$_{ax}$, they show a similar general profile but with a much reduced barrier (~1 kcal mol^{-1}) at the 300° minima indicating a much reduced $n_O \rightarrow \sigma^*_{CC}$ hyperconjugative contribution (Figure S8). The reduced barrier is much more consistent with the smaller difference (less than 1 kcal mol^{-1}) in electrostatic energy stabilisation between the two possible $CH_{ax}\cdots OC$ NCHBs in these conformers (Figure 3).

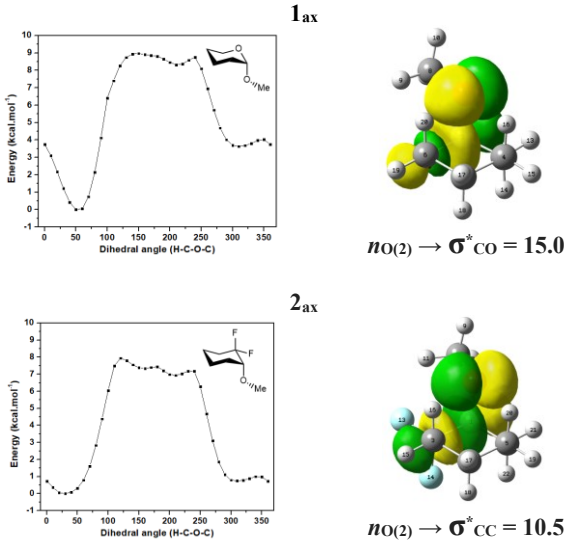

Figure 8. Calculated potential energy curves (left) obtained by scanning the H-C-O-Me dihedral angles in 10° increments at the M06-2X/aug-cc-pVTZ theoretical level for **1**$_{ax}$ and **2**$_{ax}$. $n_O \rightarrow \sigma^*_{CO}$ and $n_O \rightarrow \sigma^*_{CC}$ hyperconjugative interactions (right) are also shown together with their energy stabilization in kcal mol^{-1}.

The axial conformer of 3-methoxytetrahydropyran **13**$_{ax}$ offers an interesting contrast (Figure S8). It can form only one weak $CH_{ax}\cdots OC$ NCHB and it has weaker $n_O \rightarrow \sigma^*_{CC}$ stabilisation (7.8 kcal mol^{-1}) when compared to **1**$_{ax}$ (15.0 kcal mol^{-1}) and **15**$_{ax}$ (16.0 kcal mol^{-1}) and thus there is a lower barrier (~2 kcal mol^{-1}) between the 50° and 300° minima, again highlighting an important role for hyperconjugation in the *exo*-anomeric effect in systems such as **1**$_{ax}$ and **15**$_{ax}$.

Conclusions

The outcomes here confirm that electrostatic $CH_{ax}\cdots OC$ NCHB interactions are the dominant contributor to an axial preference for fluoro-methoxycyclohexane analogues **2**, **4**, **5** and **8** when ring CH_2 groups are replaced by CF_2 at positions 2, 4 and 6. NCHB interactions become more important with increasing CF_2 substitution because the C3-H_{ax} and C5-H_{ax} hydrogen atoms become increasingly electropositive. However, an unexpected outcome was the observation that when fluorine atoms are placed at geminal equatorial orientations at C3-$F_{eq}H_{ax}$ and C5-$F_{eq}H_{ax}$ such as in cyclohexanes **9-12**, the 'pseudo' anomeric effect diminishes as the geminal H_{ax} atoms are less electropositive. Progression of the analysis to the more ubiquitous oxa-heterocycles demonstrates that the anomeric preferences for **16** with two anomeric oxygens, and then again with **18** with three, becomes significantly less than the anomeric prototype 2-methoxytetrahydropyran **1**. Both hyperconjugation and NCHB ($CH_{ax}\cdots OC$) interactions are weaker than those found in the fluoroanalogues. This arises because the ring oxygen atoms donate electrons to the H_{ax} atoms through $n_O \rightarrow \sigma^*_{CHax}$ hyperconjugative interactions, making these oxygens poorer anomeric donors and the axial hydrogens less positively charged, and thus poor NCHB donors. None-the-less these electrostatic interactions dominate the hyperconjugation contribution in dictating an axial preference but progressively less with increasing oxygen atoms. These observations support the current revision of the anomeric effect which argues an increasing role for electrostatics.[11,12] Finally, hyperconjugation was shown to be the most significant contributor to the *exo*-anomeric effect in which $n_O \rightarrow \sigma^*_{CO}$ or $n_O \rightarrow \sigma^*_{CC}$ interactions stabilise a *gauche* geometry and where the $CH_{ax}\cdots OC$ NCHB interactions are relatively weaker.

Conflicts of interest

There are no conflicts to declare.

Acknowledgements

We thank FAPESP, CONFAP and The UK Academies FAPESP for a São Paulo International Research Collaboration (FAPESP #2019/05028-7). FAPESP is also gratefully acknowledge for an undergraduate fellowship to BAP (#2019/03855-3), and a Young Research Award to RAC (#2018/03910-1). CENAPAD-SP, CESUP and SDumont are acknowledged for computational resources used in the theory calculations. We also thank EPSRC for a grant (EP/S030506/1).

Notes and references

1 E. Juaristi, R. Notario, *J. Org. Chem.,* 2016, **81**, 1192–1197.
2 M. P. Freitas, *Org. Biomol. Chem.,* 2013, **11**, 2885–2890.
3 D. Nori-Shargh, S. N. Mousavi, R. Tale, H. Yahyaei, *Struct. Chem.,* 2016, **27**, 1753–1768.
4 N. Hasanzadeh, D. Nori-Shargh, M. Farzipour, B. Ahmadi, *Org. Biomol. Chem.,* 2015, **13**, 6965–6976.
5 E. Juaristi, R. Notario, *J. Org. Chem.,* 2018, **83**, 10326–10333.
6 Y. Mo, *Nat. Chem.*, 2010, **2**, 666–671.
7 R. U. Lemieux, *Pure Appl. Chem.,* 1971, **25**, 527–548.
8 V. G. S. Box, *Heterocycles*, 1990, 1157–1181.
9 V. G. S. Box, *J. Mol. Struct.,* 2001, **569**, 167–178.
10 V. G. S. Box, *Heterocycles*, 1991, 795–807.
11 O. Takahashi, K. Yamasaki, Y. Kohno, K. Ueda, H. Suezawa, M. Nishio, *Carbohydr. Res.,* 2009, **344**, 1225–1229.

12 K. B. Wiberg, W. F. Bailey, K. M. Lambert, Z. D. Stempel, *J. Org. Chem.,* 2018, **83**, 5242–5255.

13 M. E. Bushbeck-Alvarado, G. Hernández-Fernández, J. Hernández-Trujillo, F. Corés-Guzmán, G. Cuevas, *J. Phys. Org. Chem.*, 2018, **31**, e3793.

14 R. C. Johnston, P. H. Y. Cheong, *Org. Biomol. Chem.,* 2013, **21,** 5057–5064.

15 S. Ghosh, S. Wategaonkar, *J. Indian Inst. Sci.,* 2020, **100**, 101–125.

16 E. D. Glendening, J. K. Badenhoop, A. E. Reed, J. E. Carpenter, J. A. Bohmann, C. M. Morales, C. R. Landis, F. Weinhold, F. NBO 7.0. *(Theoretical Chem. Institute, Univ. Wisconsin, Madison, WI, 2018); http//nbo7.chem.wisc.edu/*.

17 R. F. W. Bader, *Atoms in Molecules: A Quantum Theory*; Claredon: Oxford, 1990.

18 E. R. Johnson, S. Keinan, P. Mori-Sánchez, J. Contreras-García, A. J. Cohen, W. Yang, *J. Am. Chem. Soc.,* 2010, **132**, 6498–6506.

19 B. A. Piscelli, W. Sanders, C. Yu, N. Al Maharik, T. Lebl, R. A. Cormanich, D. O'Hagan, *Chem. - A Eur. J.,* 2020, 1–7.

20 F. Weinhold, C. R. Landis, *Discovering Chemistry with Natural Bond Orbitals*; John Wiley & Sons, Inc.: New Jersey, 2012.

21 Badenhoop, J. K.; Weinhold, F. Natural Bond Orbital Analysis of Steric Interactions. *J. Chem. Phys.* **1997**, *107* (14), 5406–5421.

22 L. E. Chirlian and M. M. Francl, *J. Comput. Chem.*, 1987, **8**, 894–905.

23 C. M. Breneman and K. B. Wiberg, *J. Comput. Chem.*, 1990, **11**, 361–373

24 A. V. Marenich, S. V. Jerome, C. J. Cramer and D. G. Truhlar, *J. Chem. Theory Comput.*, 2012, **8**, 527–541.

25 . U. C. Singh and P. A. Kollman, *J. Comput. Chem.*, 1984, **5**, 129–145.

26 B. H. Besler, K. M. Merz and P. A. Kollman, *J. Comput. Chem.*, 1990, **11**, 431–439.

27 R. S. Mulliken, *J. Chem. Phys.*, 1955, **23**, 1833–1840.

29 D. Cremer, J. A. Pople, *J. Am. Chem. Soc.*, 1975, **97**, 1354-1358.

28 E. J. Cocinero, P. Çarçabal, T. D. Vaden, J. P. Simons, B. G. Davis, Nature, 2011, **469**, 76 - 80